Comparison of Tracking Performance and Robustness of Simplified Models of Multirotor UAV's Propulsion Unit with CDM and PID Controllers (with anti-windup compensation)

Wojciech Giernacki, Talar Sadalla

Institute of Control and Information Engineering, Poznan University of Technology, ul. Piotrowo 3A, 60-965 Poznań, Poland, (e-mail: wojciech.giernacki@put.poznan.pl)

Abstract: The main aim of this article is to compare two tuning methods, namely CDM (Coefficient Diagram Method) and PID (Proportional-Integral-Derivative) based on pole placement with five different anti-windup compensators. For three example models, commonly used in multirotor unmanned aerial vehicles, presenting different physical and dynamical properties (e.g. thrusts), authors proposed simplified mathematical models (first-order inertial model with time-delay). First model was obtained by estimation based on *MATLAB System Identification Toolbox*, second was estimated with graphical method and empirical selection of parameters. Thrust characteristics were recorded on the test stand and used for model parameterization. Tuning methods (CDM algorithm and PID pole placement) are briefly described in further part of this paper in the context of tracking performance and tolerance to parameter uncertainty. The comparison was based on two integral quality indices types: IAE (Integral of Absolute Error) and ISE (Integral of Squared Error).

Keywords: Coefficient Diagram Method, anti-windup compensator, pole placement, PID control, propulsion unit simplified model, thrust controller, robust control.

1. INTRODUCTION

Recently science observes increased interest in multirotor unmanned aerial vehicles used for different purposes – specification in (Austin, 2010). This interest motivates engineers to develop new and more complex models. Developmental research (Nawrat and Kuś, 2013; Lozano et al., 2014; Valavanis et al., 2007) is focused on modern sensors, electronics, autonomy, as well as on low-level layers of control responsible for stabilizing the robot and harnessing its dynamics. There are many papers describing how to ensure appropriate thrust and torque (Magsino et al., 2013; Bouabdallah et al., 2004) but all of them focus mainly on coupling lightweight and mechanically durable construction with selected propulsion configuration. Classic constructions of multirotor aerial robots dominate. Those are based on cross-frame to which the propulsion units are connected – most commonly four, six or eight single drive units, and in the last years often eight (Peng, et al., 2015) or six (Chen et al., 2014) in coaxial system configuration. The main advantage of coaxial units is a better thrust to robot dimensions ratio. Propulsion unit selection is another area of research (Bondyra et al., 2016) and even though it is not taken into account in this paper authors selected three different sets of propulsion units (different thrust, power consumption, *etc*.) to show the performance of controllers presented in further section of the article. The perspective of robot's limited sources of power (large and heavy energy cells in relations to entire construction) obliges to provide the appropriate „energy management" to increase robot's application area. To use this solution, it is necessary to implement effective control algorithms. In not expensive, commercial multirotors (used for entertainment and photography), control systems are based on manual control of the robot orientation (Euler angles or Tait-Bryan angles) in local coordinate system ("body frame") and setting thrust value. The stability loop is implemented for each rotation angle (Pitch, Roll, Yaw) in *x,y,z* reference system and for thrust (most frequently with PID controllers). The computation algorithm (commonly called „mixer") enables to perform certain manoeuvres by changing the rotation speed of each propulsion unit. In more complex solutions (Valavanis et al., 2007) cascade control systems are used. The inner loop of the cascade system (robot orientation) is based on three orientation controllers towards *x,y,z* axis and the outer loop (robot positioning) is based on three controllers responsible for robot positioning in *X,Y,Z* reference system ("Earth system") with regard to the observer.

Despite the accurate method of control, the main issue is often forgotten: propulsion unit construction. That is the key to success which ensures appropriate rotational speed in relation to expected thrust and propeller torque (Magsino et al., 2013). It seems that simulating the propulsion units (most common the brushless DC motors) is not the challenge, but propellers spinning with high speed (few to over a dozen thousands rotations per minute) and the influence of aerodynamics is. This is the reason why the dynamics of the propulsion units is approximated by simplified linear models as well as with multidimensional nonlinear models (Szafrański, 2015). Authors focus on aerodynamic effects, that the flying robot construction is submitted to (propulsion units which cause these effects), and can be expressed in dynamical model of UAV. By implementing additional

measurements (rotational speed, current, *etc*. in every unit) it is possible to propose additional control systems (rotational speed, thrust, torque control system, *etc*.) from Fig.1 for simplified propulsion unit models. Thus, we make sure that the declared parameters, despite any disturbances, are achieved (mostly the step-like changes of the wind blast, *etc*.)

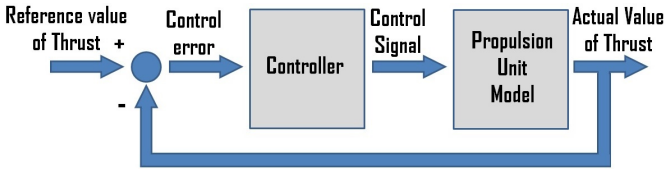

Fig. 1. Block diagram of proposed closed-loop control system of thrust (for particular propulsion unit).

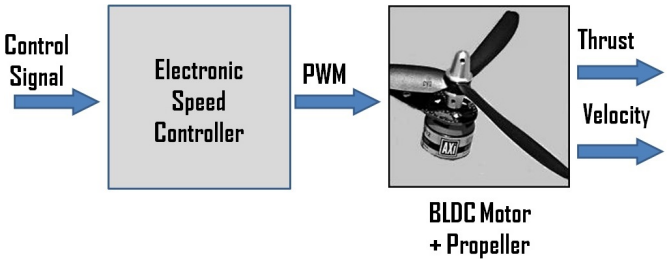

Fig. 2. Block diagram of propulsion unit with signals.

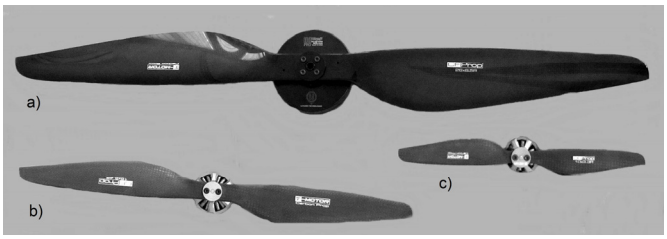

Fig. 3. Propulsion units: a) U8 Pro + 26" propeller, b) MN4014 + 16" propeller, c) MN3110 + 10" propeller.

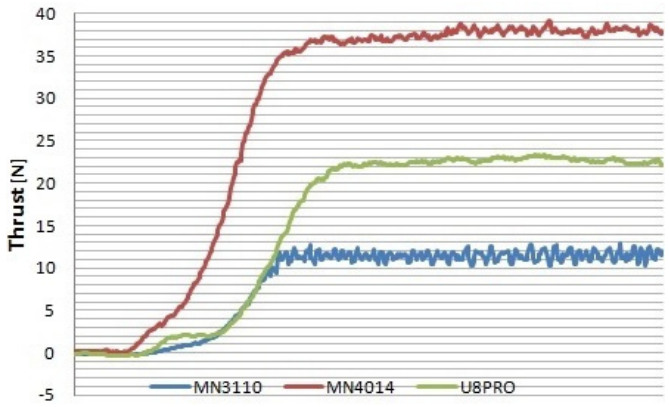

Fig. 4. Step responses of propulsion units with MN3110, MN4014 and U8PRO BLDC motors (as samples function).

In this paper authors present the effective control of desired thrust that is produced in system precisely called: propulsion unit (brushless DC motor with propeller embedded directly on the shaft) drove by proper voltage input modulation from ESC system (Electronic Speed Controller) – Fig.2 (Giernacki, et al., 2016). In many papers speed control loop is commonly used (Magsino, et al., 2013) because of the simplicity of measurements made directly on the robot in real time. It is worth noting that speed and thrust measurements are not the subject of this paper but their practical aspect. Methodology and considerations can be successfully generalized and transferred on the aforementioned speed control systems (if one uses different characteristics of the propulsion unit instead of presented equivalents of thrust). Prospective results of simulations (presented briefly in (Giernacki, et al., 2016)) provided a closer look at this topic and allowed to perform more comprehensive research.

Article is organized as follow – section II presents the analysed models, as well as the methodology explaining how they were constructed, description of necessary data acquisition and parameters estimation. Section III is divided into two subsections that describe two types of thrust control systems: CDM (Coefficient Diagram Method), robust to parameter uncertainty, and PID based on pole placement tuning method (without and with anti-windup compensation). The issues of windup compensation problem, robustness to parameter uncertainty and control quality are discussed in section IV based on comparison of those two tuning methods. Section V features conclusions and further research.

2. PROPULSION UNIT MODELS

2.1 Data acquisition

On a specially prepared test stand (more comprehensive description in (Bondyra et al., 2016)) for different quadrotor and coaxial quadrotor generation such as *Falcon* and *Dropter* realized at *Institute of Control and Information Engineering* at *Poznan University of Technology* many simulations were performed for important data acquisition. This inspired creating models of propulsion unit systems used in unmanned aerial vehicles (from the simplified linear models to complex multidimensional nonlinear models that include electric and aerodynamic aspects) and designing different types of controllers and tuning methods. For this purpose three different types of propulsion units from *T-Motor* company were applied on the test stand (Fig.3):

- energy efficient U8-16 PRO BLDC motor with 26" propeller – nominal rotation speed of about 2500 rpm, up to 2 kg of thrust and 300 W of maximum power consumption,

- maximizing thrust MN4014 BLDC motor with 16"x5.4" propeller – up to 3 kg of thrust, 900 W of power consumption,

- MN3110-15 BLDC motor with small propeller size 10"x3.3" – nominal rotation speed of 11544 rpm, up to 1.03 kg of thrust and 481 W of maximum power consumption.

After calibration of the test stand for each propulsion unit ten trials of thrust force were recorded on dedicated software: *DYNO Terminal*. The PWM step-like changes of voltage were the input of the system in the range from 0% to 98% and the system response was collected as the thrust force characteristics. The average response from ten trials is shown in Fig.4. Authors recorded one test of changing PWM and response signals in time (Fig.5). This data were used for models validation.

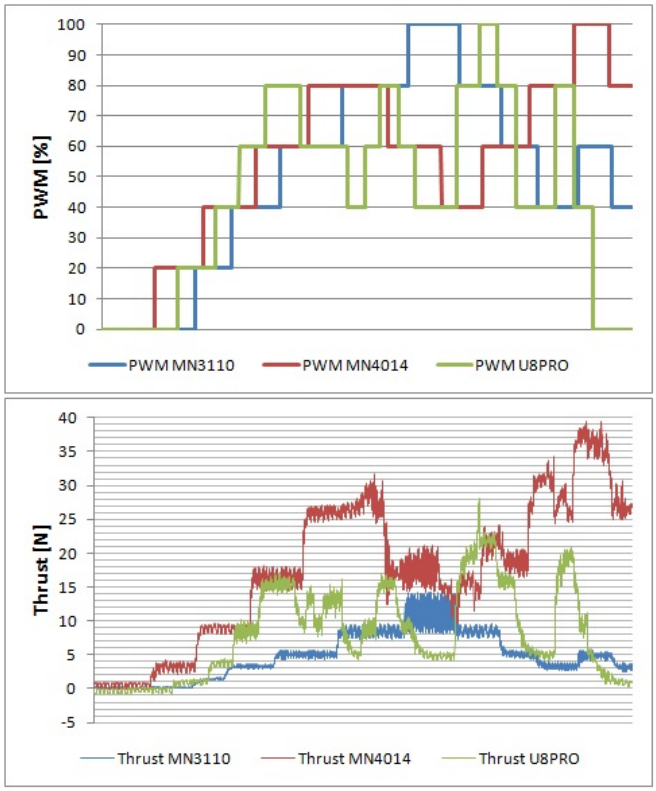

Fig. 5. Thrust responses of MN3110, MN4014 and U8PRO BLDC motors models for PWM input function.

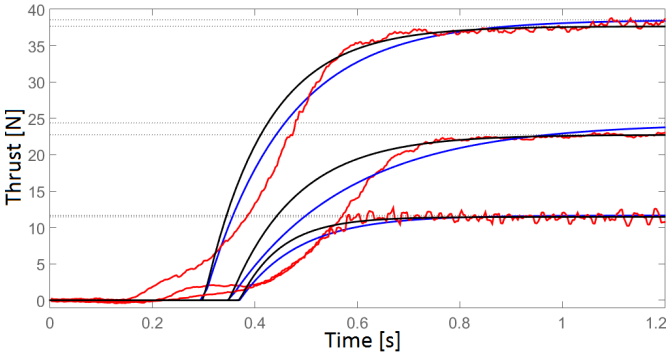

Fig. 6. Step responses (from the top: MN4014, U8PRO, MN3110) of real propulsion units (red), simplified models obtained via graphical method (black) and by estimation of models created with *MATLAB's System Identification Toolbox* (blue).

2.2 Parameter estimation

The range of useful thrust forces used during the flight of the multirotor robots does not exceed 70% of the maximum value (above the value of thrust force requires bigger power consumption). The analysis of the recorded data from Fig.4 with estimation of the parameters (with validation on data set from Fig.5) enables to create linear models of propulsion units – namely, a first-order inertial model with time-delay (Table 1). In this case two different estimation methods were used. First was based on toolbox from *MATLAB 2015a* software – *System Identification Toolbox*. The second was based on graphical analysis of step responses from which specific dynamical parameters were collected. In each considered case, the graphical method was more precise in estimation of the real plant than the estimation of the model with the use of *MATLAB System Identification Toolbox* (Fig.6).

To simplify the computations, the exponential form of time-delay was approximated by first-order linear model. Because Padé approximation creates problem of non-minimum phase system (zero in the numerator of the closed-loop transfer function) it was assumed that the time-delay approximation takes the form of: $e^{-sT_o}=j_0/(h_1 s+h_0)$ (assuming that $T_0<0.5$), where: $j_0=1$, $h_0=1$. Results are presented in Table 1.

Table 1. Parameter estimation and proposed models $G_p(s)$ of propulsion units (models used in the paper are marked in grey).

MN3110	MN4014	U8PRO
IDENT		
$\frac{11.65e^{-0.37s}}{0.115s+1}$	$\frac{38.55e^{-0.3s}}{0.1585s+1}$	$\frac{24.37e^{-0.35s}}{0.2301s+1}$
Graphical		
$\frac{11.46e^{-0.37s}}{0.08s+1}$	$\frac{37.65e^{-0.3s}}{0.12s+1}$	$\frac{22.74e^{-0.35s}}{0.13s+1}$
Padé		
$\frac{-11.46s+61.94}{0.08s^2+1.43s+5.4}$	$\frac{-37.65s+251}{0.12s^2+1.8s+6.7}$	$\frac{-22.74s+130}{0.13s^2+1.74s+5.7}$
Approximation: $e^{-sT_0}=\frac{j_0}{h_1 s+h_0}$		
$\frac{11.46}{(0.08s+1)^2}$	$\frac{37.65}{(0.12s+1)^2}$	$\frac{22.74}{(0.13s+1)^2}$

3. SYNTHESIS OF CONTROL SYSTEMS

In the case of control system synthesis the type of notation and model structure determine the type of controller, control law and tuning method – see (Raptis and Valavanis, 2011). With reference to control systems of multirotor unmanned aerial vehicles, their multilayer and cascade characteristics, besides the simplified linear mathematical model, it is necessary to use fast and universal controllers. Those requirements can be achieved with PID controllers – still commonly used (Flores et al., 2012; Li & Li, 2011; Bouabdallah, 2004). However, their main advantage – the universality of usage is not always equal with control quality. In most situations lack of optimization criteria or other meaningful aspects causes difficulties in control quality and this problem is described in further part of this paper. The most important aspect is the influence of the integral part of controller when the control signal reaches saturation limit. Tuning PID type controller with different methods (Ziegler-Nichols or pole placement used in this paper) does not consider this aspect – therefore, it is necessary to use windup compensators (Sadalla and Horla, 2015a). Another important aspect concerning control quality is the robustness of the controller to parameters model uncertainty. Even if the most complex methods are used, the obtained model will always more or less differ from its real equivalent. This aspect is analysed in this paper. To achieve reference of results, PID type controllers (with antiwindup compensation) tuned with pole placement method were compared to results achieved with coefficient diagram

method, which is also classified as polynomial control (tuning based on placing the poles of the closed-loop characteristic equation (Manabe, 1998)). Necessary information with reference to both methods used and important literature are presented in the next *Section*.

3.1 Coefficient Diagram Method

The CDM algorithm is based on the idea of relationship between obtained closed-loop system time characteristics and placement of characteristic polynomial poles on the complex plane *s* (Manabe, 1998). It is worth noting, that this control design method objective is used to easily obtain a good controller with minimum user effort (Coelho et al. 2014). From the user point-of-view, the main feature of CDM is its simplicity. If the system model is known (transfer function), the control designer only needs to define two things: the value of time constant equivalent and the controller order for the expected system disturbance shape. Then the controller's transfer function is automatically obtained via algebraic method (analogically to pole placement) (Coelho et al., 2014). The simplicity of procedure, stability assurance in the first iteration of algorithm, possibility of use of special tool (coefficient diagram – more in (Manabe and Kim, 2000)) to analyse the dynamics, stability and robustness of the system, proves that CDM method is a useful and practical method of PID type controller tuning, especially if it is considered to be used in aerial systems that are known for high dynamics (Budiyono et al., 2009). Full description of this method, necessary mathematical formulas and tuning algorithm can be found in (Manabe, 2005; Coelho et al., 2014; Bir and Tibkin, 2009).

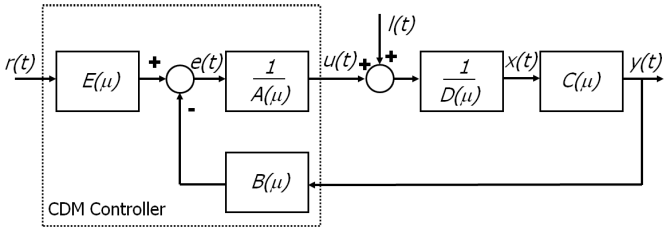

Fig. 7. Block diagram of CDM closed-loop system.

The synthesis of controller for the system from Fig.7 starts from the notation of plant model expressed in the time domain (regarding (Coelho et al., 2014)) – by the use of μ operator defined in (1):

$$\frac{d^i}{dt^i} = \mu^i . \tag{1}$$

A general linear differential equation with constant coefficient a_i and b_j, for $i=0,...,n$ and $j=0,...,m$, with the following generic structure

$$a_0 y(t) + \sum_{i=1}^{n} a_i \frac{d^i y(t)}{dt^i} = b_0 u(t) + \sum_{j=1}^{m} b_j \frac{d^j u(t)}{dt^j} \tag{2}$$

can assume an alternative formulation using μ operator as shown:

$$y(t)\left(a_0 + \sum_{i=1}^{n} a_i \cdot \mu^i \right) = u(t)\left(b_0 + \sum_{j=1}^{m} b_j \cdot \mu^j \right). \tag{3}$$

This representation resembles a polynomial in μ with a_i and b_j as coefficients (of $A(\mu)$ and $B(\mu)$ polynomials) and n and m as their orders. The system differential equation may be written in a more compact way as follows:

$$A(\mu) \cdot y(t) = B(\mu) \cdot u(t) \tag{4}$$

where the dot operation represents the product between each polynomial term and related signal.

In CDM controller design (Coelho et al., 2014), the pre-filter $E(\mu)$ is a zero-order polynomial and its only coefficient is computed in order to achieve closed-loop zero steady state error. Model of plant dynamics consist of two polynomials: $C(\mu)$ and $D(\mu)$. For the sake of simplicity, let the order of both polynomials $A(\mu)$ and $B(\mu)$ be equal to m and the order of both polynomials $C(\mu)$ and $D(\mu)$ equal to n (even if some higher order coefficient of $B(\mu)$ must be set to zero). Thus, the $m+n$ order characteristic polynomial $P(\mu)$ of closed-loop control system may be written as follows:

$$P(\mu) = A(\mu) \cdot D(\mu) + C(\mu) \cdot B(\mu). \tag{5}$$

Characteristic polynomial from (5) may be rewritten as:

$$P(\mu) = \sum_{i=0}^{n+m} p_i \cdot \mu^i . \tag{6}$$

Let us define two additional figures: the stability index, denoted by γ_i for $i=1,...,(n+m)-1$ and the predominant time constant τ. Both are described in further detail in (Manabe, 1998) and presented hereafter in (7) and (8):

$$\gamma_i = \frac{p_i^2}{p_{i-1} p_{i+1}}, \tag{7}$$

$$\tau = \frac{p_1}{p_0}. \tag{8}$$

Each of the characteristic polynomial coefficient p_i in (6) can be written as a function of both stability indexes and predominant time constant. Hence the (normalized) characteristic polynomial can be expressed alternatively as:

$$\frac{P(\mu)}{p_0} = \sum_{i=2}^{n+m} \left\{ (\tau\mu)^i \left(\prod_{j=1}^{i-1} \frac{1}{\gamma_j^{i-j}} \right) \right\} + \tau\mu + 1. \tag{9}$$

For Manabe's polynomial (one of the best, ready-to-use characteristic polynomial structures), the coefficients are chosen in order to have the following stability index values (Manabe, 1998):

$$\gamma_i = \begin{cases} 2.5 & if \quad i = 1 \\ 2 & if \quad i = 2,..., n+m \end{cases}. \tag{10}$$

In classic version of a pole placement method it is not specified how to obtain the desired characteristic polynomial in particular system (Coelho et al., 2014) – it is only

mentioned that it should provide stable closed-loop system. The CDM method presents a simple way to obtain such a polynomial (by just defining the desired equivalent time constant) that will provide good performance (stability, robustness and control quality). Then, having the desired characteristic polynomial, the next step is just algebra and solving a system of equations with the formulation described in (5).

Having p_0, τ and γ_i beforehand, the problem is pole-placement (Koksal and Hamamci, 2004). However, in the CDM method the Sylvester matrix structure differs from the pole placement one. It is related with the knowledge of certain coefficients $A(\mu)$ due to a priori assumptions about the type of system disturbances (consider Table 2).

Assuming the Sylvester matrix $\mathbf{A}$ has the structure represented in (12) and that the unknown polynomial coefficients, considering zero lower k coefficients of $A(\mu)$, are arranged in a vector $\boldsymbol{x}$ as expressed in (13) then the CDM controller solution is obtained by solving (11):

$$x = \mathrm{A}^{-1} \cdot p \tag{11}$$

where:

$$\mathrm{A} = \begin{bmatrix} d_m & c_m & \cdots & 0 & 0 \\ \vdots & \vdots & & \vdots & \vdots \\ d_{m-n+k} & c_{m-n+k} & & 0 & 0 \\ \vdots & \vdots & & \vdots & \vdots \\ d_0 & c_0 & \ddots & 0 & 0 \\ 0 & 0 & & d_m & c_m \\ \vdots & \vdots & & \vdots & \vdots \\ 0 & 0 & \cdots & d_0 & c_0 \end{bmatrix} \tag{12}$$

and

$$x = \begin{bmatrix} a_n & b_n & \cdots & a_k & b_k & b_{k-1} & \cdots & b_0 \end{bmatrix}^T, \tag{13}$$

$$p = \begin{bmatrix} p_{n+m} & \cdots & p_1 & p_0 \end{bmatrix}^T. \tag{14}$$

3.2 PID pole placement control with anti-windup compensation (AWC systems)

The PID pole placement method is based on comparison of the closed-loop characteristic equation and its desired form.

The model of such a system with anti-windup compensation (AWC) is presented in Fig. 8 (Giernacki, et al., 2016).

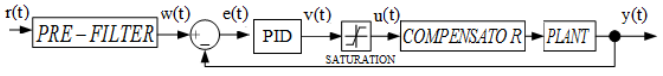

Fig. 8. *Matlab-Simulink* diagram of tracking system with time-delay.

The model of the plant $G_p(s)$ is described by transfer function:

$$G_p(s) = \frac{b_0}{a_1 s + a_0} e^{-sT_0}. \tag{15}$$

Table 2. Controller order selection as a function of signal disturbance type.

Disturbance type	$A(\mu)$ degree	$B(\mu)$ degree	$P(\mu)$ degree	Condition
None	n-1	n-1	2n-1	-
Step	n	n	2n	a_0=0
Impulse	n-1	n-1	2n-1	-
Ramp	n+1	n+1	2n+1	a_0=0 a_1=0
k order	n+k-1	n+k-1	2n+k-1	a_0=0 … a_k-1=0

The gain of the model is b_0 and T_0 is a time-delay. All coefficients are assumed known. The PID controller takes the form of (16):

$$G_{PID}(s) = \frac{k_d s^2 + k_p s + k_i}{s} \tag{16}$$

and its parameters should be tuned *off-line* with respect to open-loop transfer function (17) as below:

$$G_o(s) = \frac{\mathrm{k}_d s^2 + k_p s + k_i}{s} \cdot \frac{b_0}{a_1 s + a_0} e^{-sT_0}. \tag{17}$$

In order to streamline the derivation of the closed-loop transfer function, a first-order approximation of time-delay (18) is assumed as follows:

$$e^{-sT_0} \approx \frac{j_0}{h_1 s + h_0}. \tag{18}$$

Now, the closed-loop characteristic polynomial is compared to its desired form (left side of (19)) with arbitrary chosen coefficients: am_3, am_2, am_1 and am_0), forming Diophantine equation with approximation of the delay, and is given as:

$$\begin{aligned} am_3 s^3 + am_2 s^2 + am_1 s + am_0 = \\ a_1 h_1 s^3 + \\ (b_0 k_d j_0 + a_1 h_0 + a_0 h_1) s^2 + \\ (a_0 h_0 + b_0 k_p j_0) s + b_0 k_i j_0 \end{aligned}. \tag{19}$$

For the pole placement problem (Aström, 2002) after computations, the solution of this Diophantine equation is:

$$\begin{aligned} k_i &= \frac{am_0}{b_0 j_0} \\ k_p &= \frac{am_1 - a_0 h_0}{b_0 j_0} \\ k_d &= \frac{am_3 - a_1 h_1 - a_0 h_1}{b_0 j_0} \end{aligned}. \tag{20}$$

The cut-off level of the computed control signal $v(t)$ (Fig. 8) set at $\pm\alpha_{min}$ allows asymptotic tracking in the closed-loop system and is used to give relative measure of constraints hardness. After comparison to the desired characteristic equation the requirements for the compensator parameters are as follows: j_0=1, h_1=am_3a_1, h_0=1. According to (20)

the primary meaning of time-delay approximation model is preserved but after solving the Diophantine equation, there is a possibility to place the poles of the closed-loop system in chosen locations (Giernacki, et al., 2016).

In order to cancel its zero-dynamics a pre-filter is added in series with the closed-loop system and modelled by the transfer function:

$$G_F(s) = \frac{k_{\text{filter}}}{k_d b_0 s^2 + k_p b_0 s + k_i b_0}, \tag{21}$$

where k_{filter} is a pre-filter gain. The main purpose of this filter is to decrease the speed of transients and reduce the probability of consecutive re-saturations of control signal.

Five different anti-windup compensators are listed to enable authors to analyse the impact of AWC on the control quality.

A short description of each is presented below:
-Tracking system with limitation of integrator (AWC1) - the main disadvantage of this type of compensator is that the integral part of the controller can be stopped even if the signal *v(t)* is not saturated,

-Tracking system with limitation of integrator with error signal *e(t)* (AWC2) - this method is based on difference between reference signal *r(t)* and the output signal *y(t)* which is fed to the integrator. If the signal *v(t)* and *u(t)* resaturates then the integration should be stopped,

-Tracking system with control signal conditioning (AWC3)

The third compensation method is described by:

$$e_i(t) = e(t)k_i + \Delta u(t) K_f T_N, \tag{22}$$

where *e(t)* is the difference between reference signal *r(t)* and *y(t)* and $\Delta u(t)$ is the difference between unsaturated *v(t)* and saturated control signal *u(t)* multiplied by known coefficients K_f and T_N.

-Tracking system with dead-zone of control signal (AWC4) - in the system with AWC4 large initial values of unsaturated control signal *v(t)* are caused by proportional and derivative part of the controller due to step changes of the reference signal *r(t)*. The integral part is not able to compensate for changes fast enough and this problem is eliminated by adding another saturation block to *P* and *D* elements of the controller,

-Tracking system with external reset of integrator (AWC5) - the last system is based on resetting the integral part of controller whenever the control signal *v(t)* exceeds the given limit. The range of dead-zone to which the control signal is fed is equal to the double cut-off limit in constrained control signal *u(t)*.

More comprehensive information and diagrams of the anti-windup compensator can be found in (Sadalla and Horla, 2015a, Sadalla and Horla, 2015b).

4. SIMULATION TESTS

Complex analysis of tracking and robustness quality in systems with PID and CDM controllers was performed. The main purpose was not the direct comparison between both methods but the general analysis and further utilization of results.

4.1 Tracking performance

The first-order inertial models with time delay presented in Table 1 (approximation based on (18)), were implemented in *MATLAB 2015a/Simulink* (standard parameters configuration) with tuning methods mentioned in *Section 3*. To evaluate performance integral of absolute error (IAE) and integral of squared error (ISE) indices have been used.

In the first analysis tracking performance of square signal (thrust force) for CDM controller was performed for simulation time of 9 seconds (Fig.9) in the presence of step type disturbances that had an impact on the model. Another aspect that was analysed was the level of control signal amplitudes. It can be noted from the recorded data that similar raising times were achieved for each of the three propulsion units (each time the expected values of time constant τ were achieved exactly as they were declared in CDM tuning procedure). However, different effectiveness of disturbances damping was observed. For the most dynamical system (MN4014) it can be noted that there are high overshoots that the controller manages in a proper way.

In the second analysis (just as in previous one) six systems with PID controller based on pole placement tuning method and with: AWC0 (model without windup compensation), AWC1-AWC5 (model with windup compensation methods that were described in *Section 3*) were analyzed. The saturation limit of the control signal for AWC1, AWC3, AWC4 and AWC5 was set to ±1 and for AWC2 ±0.1. For AWC3 system there are two additional parameters: $K_f = 1$ and $T_N = 0.1$. Further description of these parameters can be found in (Hyppe, 2006) and it is omitted here for undisturbed presentation of work results.

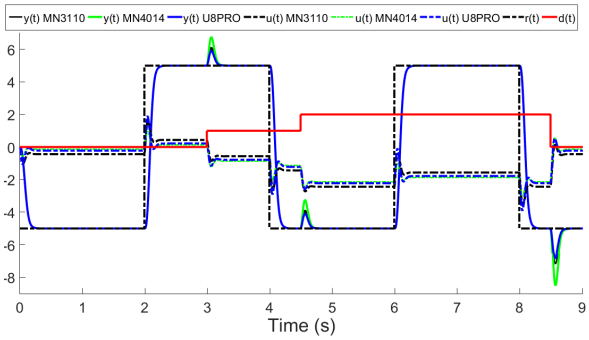

Fig. 9. Reference signal *r(t)*, control signal *u(t)*, output signal *y(t)* and disturbance signal *d(t)* for the control systems with CDM controllers.

Current research is the extension of previous presented in (Giernacki, et al., 2016), where it was concluded that using proper windup compensation method with pole placement tuning method of PID controller leads to decrease of disturbance damping. However, the consequences are that it lowers the dynamics of the closed-loop system (increase of steady-state time response). Results presented in Fig.10

show the subtle differences between each type of AWC according to the system without compensation (AWC0).

Table 3. Integral quality indices IAE and ISE for propulsion unit models (AWC0-AWC5).

	AWC 0	AWC1	AWC 2	AWC3	AWC 4	AWC 5
	MN3110					
IAE	18.096	11.746	11.944	12.236	15.667	11.920
ISE	87.337	57.177	55.149	61.073	75.595	58.016
	MN4014					
IAE	13.844	12.650	12.559	12.846	13.635	12.749
ISE	91.639	76.159	71.219	78.859	89.167	77.170
	U8PRO					
IAE	16.003	15.515	15.423	15.638	15.959	15.585
ISE	111.57	104.247	97.688	105.327	110.86	105.13

Table 3 presents integral quality indices. In each of the three propulsion units the most effective was the AWC1 system which has the fastest output response and good disturbances damping.

4.2 Robustness analysis for parameters uncertainty

Authors tried to find the answer to the question: how will the controllers (CDM and pole placement with AWC1) manage parameter uncertainty of the models? Talking about placing poles at specific point is just theorising this aspect because creating simplified model requires approximation and it affects tracking performance quality of a real plant if the controller is tuned for its simplified model.

First test was focused on recording the integral quality indices IAE and ISE (Fig.11) for changing a_1 and T_0 values of propulsion units models with CDM controller (analogically to model from subsection 4.1). Parameters T_0 and a_1 were changed in specified range +/- of nominal value of each unit parameters.

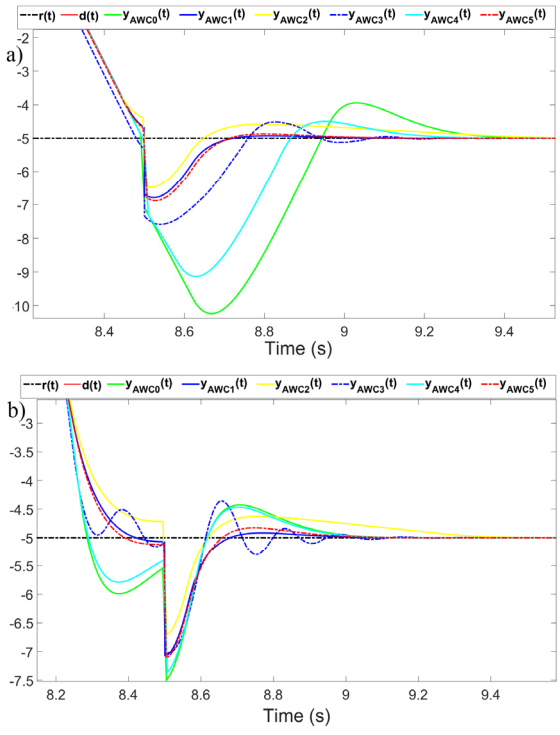

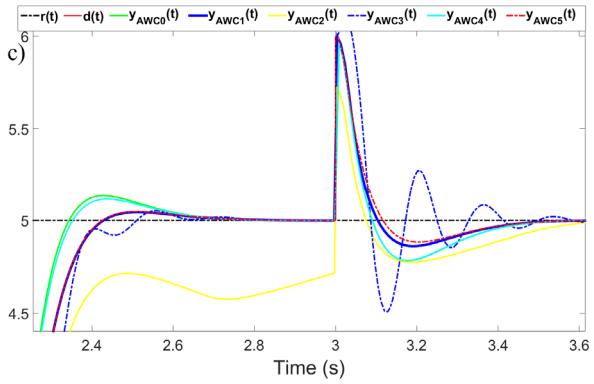

Fig. 10. Zoom of time courses for control systems with PID controllers and a) MN3110, b) MN4014, c) U8PRO propulsion unit plant models.

The controller tuned with coefficient diagram method is robust to changes of a_1 parameter (time constant of the first-order inertia plant). However, its effectiveness decreases with increasing of the time-delay parameter T_0.

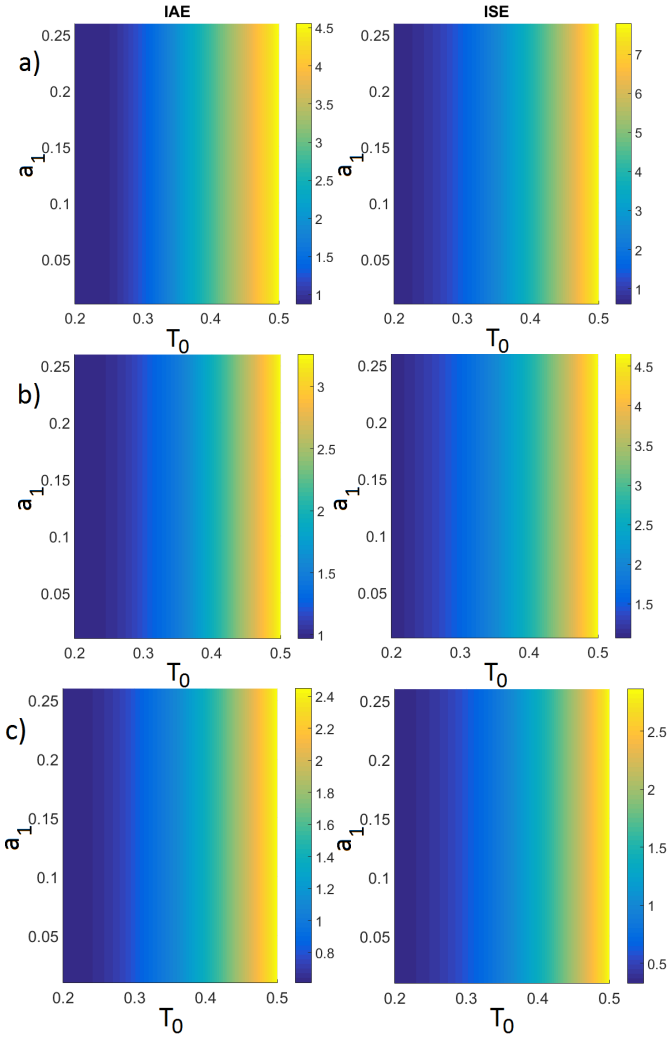

Fig. 11. Integral quality indices IAE and ISE for the change of T_0 and a_1 parameters of the propulsion unit model: a) MN3110, b) MN4014, c) U8PRO with CDM controller.

The second test was performed for systems with AWC1 model and PID controller. To verify its parametrical

robustness results have been compared to AWC0 system without anti-windup compensation, and two integral quality indices were used, defined as (23)-(24):

$$\Delta J_1 = IAE_{AWC0}(T_{0i}, a_{1j}) - IAE_{AWC1}(T_{0i}, a_{1j}), \quad (23)$$

$$\Delta J_2 = ISE_{AWC0}(T_{0i}, a_{1j}) - ISE_{AWC1}(T_{0i}, a_{1j}), \quad (24)$$

where i and j are respectively values of T_0 and a_1 in the range of their uncertainty (see Fig.12). Positive values of ΔJ_1 and ΔJ_2 correspond to the degree of robustness improvement when AWC1 system is used. Recorded values show (similarly as it was for CDM controller) high robustness for parameter a_1 uncertainty, however, the robustness of AWC1 system increases in comparison to AWC0 system and time-delay parameter T_0 increases as well. For lower time-delay values the differences are not so significant – especially for U8PRO unit. From the recorded values of ΔJ_1 and ΔJ_2 it can be noted that for smaller propeller dimensions it is more important to use anti-windup compensators – for bigger dimensions (bigger inertia) there is no meaningful improvement in robustness.

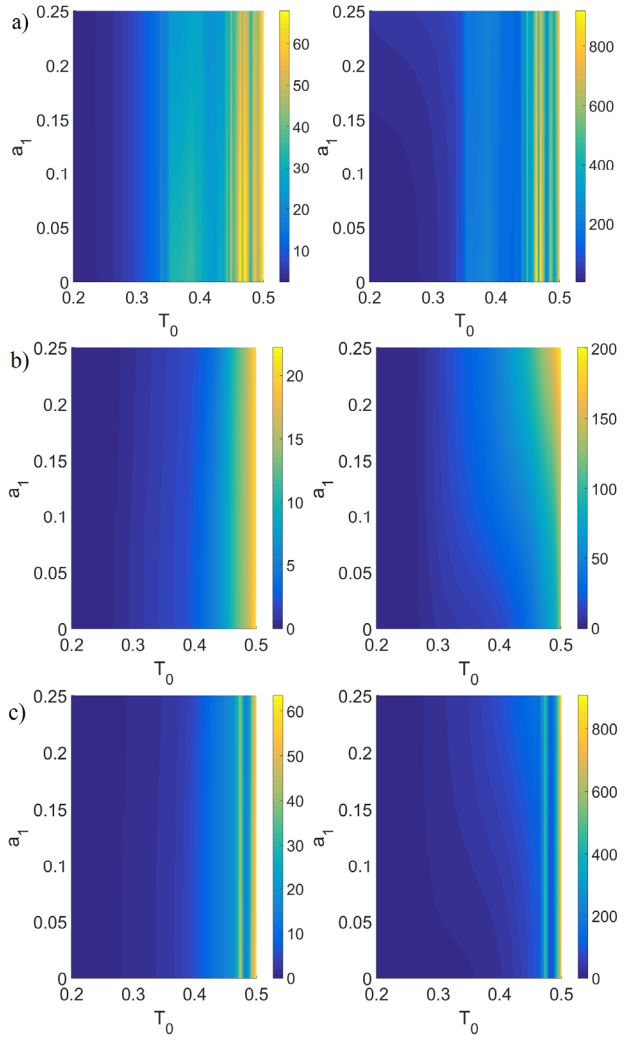

Fig. 12. Integral quality indices ΔJ_1 and ΔJ_2 for the change of T_0 and a_1 parameters of the propulsion unit model: a) MN3110, b) MN4014, c) U8PRO with PID controller (system with AWC1 related to AWC0).

Third test (analogically to the first one) verifies the robustness of CDM controller to parameter b_0 (model gain) and T_0 time-delay uncertainty. Similar results were achieved as earlier, the CDM controller is robust to uncertainty b_0 parameter (the controller tuned for nominal model tolerates gain uncertainty adjusting the output signal) – see Fig. 13.

Last test was performed for PID controller with anti-windup compensator AWC1. To verify its parametrical robustness results have been compared to AWC0 system without anti-windup compensation and two integral quality indices were used: ΔJ_3 and ΔJ_4, defined as (25)-(26):

$$\Delta J_3 = IAE_{AWC0}(b_{0i}, T_{0j}) - IAE_{AWC1}(b_{0i}, T_{0j}), \quad (25)$$

$$\Delta J_4 = ISE_{AWC0}(b_{0i}, T_{0j}) - ISE_{AWC1}(b_{0i}, T_{0j}), \quad (26)$$

where i and j are respectively values of b_0 and T_0 in the range of their uncertainty (see Fig.14). From the achieved results it can be observed, based on ΔJ_4 quality index, that AWC1 system definitely increases the effectiveness of robustness for time-delay parameter uncertainty in comparison to AWC0 system without compensation. Analogically to CDM controller, the model gain uncertainty errors are effectively compensated by controller gains.

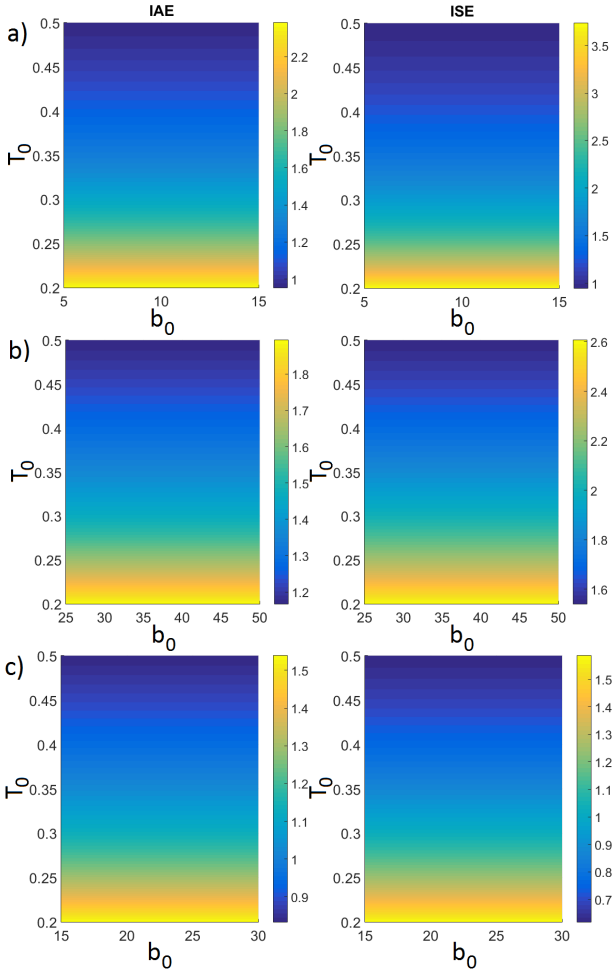

Fig. 13. Integral quality indices IAE and ISE for the change of b_0 and T_0 parameters of the propulsion unit model: a) MN3110, b) MN4014, c) U8PRO with CDM controller.

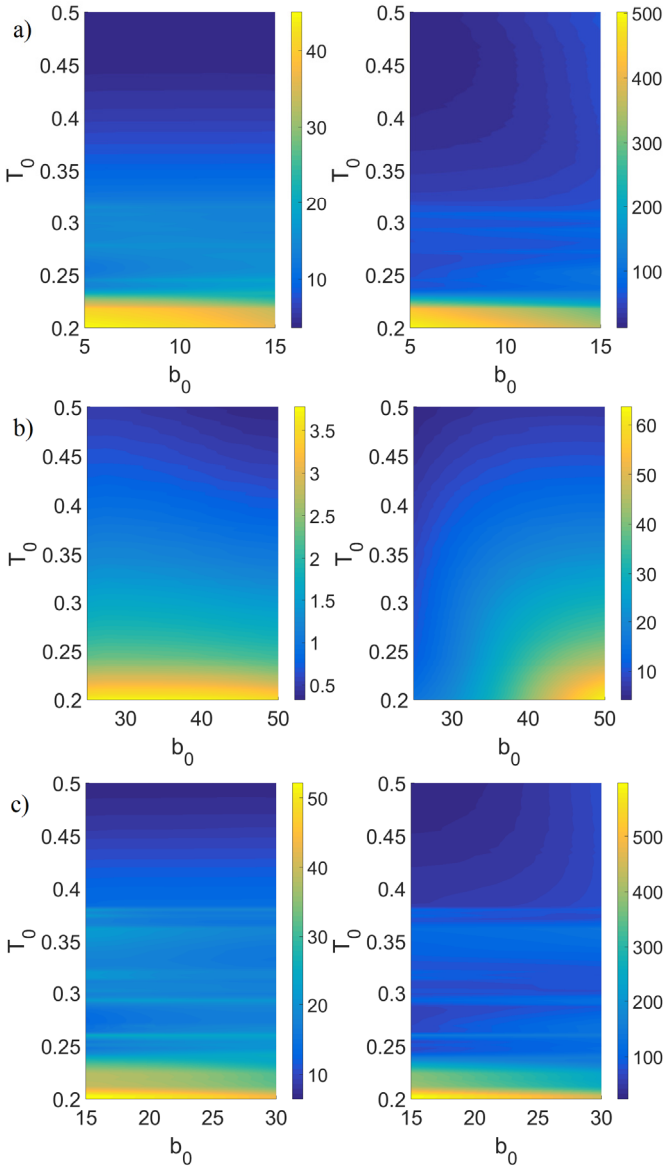

Fig. 14. Integral quality indices ΔJ_3 and ΔJ_4 for the change of b_0 and T_0 parameters of the propulsion unit model: a) MN3110, b) MN4014, c) U8PRO with PID controller (system with AWC1 related to AWC0).

5. CONCLUSIONS

The comparison of two controller tuning methods based on pole placement were presented in this article. Both of them give a possibility to solve the Diophantine equation if the structure of the model and controller is known. The main difference is the method of calculating poles of the closed-loop transfer function. It has an impact on damping disturbances, output response characteristics and parametric robustness. Those aspects were analysed and the CDM tuning method confirms that it can be used for controlling the thrust force in propulsion units that have different dynamical characteristics and are applied in multirotor aerial robots. The biggest advantage of this method is that it has fast output response after the change of reference signal but the disturbance damping (such as wind gusts) aspect needs to be improved and this requires further research.

On the other hand, pole placement for PID controllers is an effective alternative – however, it is necessary to choose the correct type of AWC and its parameters. It helps to overcome one of the most known problems with PID controllers, namely, the control signal protraction when it gets saturated. The effectiveness of control with AWC1 shows good dynamics (lower than CDM), most effective disturbances damping and high parametric robustness, which is important when applying this method in UAVs. In authors' opinion, the dynamics of steady-state time response after the change of reference signal can be improved because in this article the control was not optimized in accordance to predefined aim function (e.g. minimization of the control errors). It is worth to consider the optimization of the controller gains or to implement the non-integer controller (such as fractional PID type controller). This gives possibility to achieve two additional tuning parameters (orders of integral and derivative part of the controller). Further research will be focused on this aspect.

REFERENCES

Aström, K.J. (2002). Control System Design, *Lecture notes for ME 155A*, University of California, Santa Barbara, USA.

Austin, R. (2010). UAVs design, development and deployment, *John Wiley & Sons*, Chippenham.

Bir, A. and Tibkin, B. (2009). Digital design of coefficient diagram method. *In Proc. of 2009 American Control Conference*, pp. 2849-2854.

Bondyra, A., Gardecki, S., Gąsior, P. and Giernacki W., Performance of coaxial propulsion in design of multi-rotor UAVs, Advances in Intelligent Systems and Computing, Challenges in Automation, *Robotics and Measurement Techniques, Springer,* pp. 523-531.

Bouabdallah, S., Noth, S. and Siegwart, R. (2004), PID vs LQ Control Techniques Applied to an Indoor Micro Quadrotor, *Proceedings of the 2004 IEEE/RSJ International Conference on Intelligent Robots and Systems*, pp. 2451-2456.

Budiyono, A., Riyanto, B. and Joelianto, E. (2009). Intelligent Unmanned Systems: Theory and Applications. *Studies in Computational Intelligence, vol. 192, Springer-Verlag*, Berlin, Heildelherg.

Chen., Z., Peng, Z. and Zhang, F. (2014). Attitude Control of Coaxial Tri-rotor UAV Based on Linear Extended State Observer, *Proceedings of the 26th Chinese CDC Conference*, pp. 4204-4209.

Coelho, J.P., Giernacki, W. and Boaventura-Cunha, J. (2014). CDM Controller Order and Disturbance Rejection Ability. *International Journal of Computer, Information, Systems and Control Engineering*, 8(8), pp. 1223-1227.

Flores, G., Garcia Carrillo, L.R., Sanahuja, G. and Lozano, R. (2012). PID Switching Control for a Highway Estimation and Tracking Applied on a Convertible Mini-UAV. *Proceedings of the 51st IEEE Conference on Decision and Control*, 2012, Maui, Hawaii, USA, pp. 3110-3115.

Giernacki. W., Horla, D., Sadalla, T. and Coelho, J.P. (2016). Robust CDM and Pole Placement PID Based Thrust Controllers for Multirotor Motor-Rotor Simplified Model. *In Proceedings of 2016 International Siberian*

Conference on Control and Communications (SIBCON), Moskow, Russia, DOI: 10.1109/SIBCON.2016.7491826.

Hyppe, P. (2006). Windup in Control, *Springer*, pp. 23-27.

Koksal, M. and Hamamci, S.E. (2004). A program for the design of linear time invariant control systems: CDMCAD. *Computer Applications in Engineering*, 12(2), pp. 165-174.

Li, J. and Li, Y. (2011). Dynamic Analysis and PID Control for a Quadrotor. *Proceedings of the 2011 IEEE International Conference on Mechatronics and Automation,* Beijing, China, pp. 573-578.

Lozano, R. Colunga G.R., Guerrero, A. and Escareno, J.A. (2014), *Modeling and Control of mini UAV. HAL. archives-ouvertes.fr/hal*-00923127.

Magsino, E.R., Dollosa, C.M., Gavino, S. and Hermoso, G. (2013). Implementation of Speed and Torque Control on Quadrotor Altitude and Attitude Stability. *The Manila Journal of Science*, 8(2), pp. 9-20.

Manabe, S. (1998). The coefficient diagram method. *The 14th IFAC Symposium on Automatic Control in Aerospace*, pp.199-210.

Manabe, S. and Kim, Y. (2000). Recent Development of Coefficient Diagram Method. *Proceedings of the 3rd Asian Control Conference*, Shanghai, China, 2000.

Manabe, S. (2005). Coefficient diagram method in MIMO application: An aerospace case study. *Proceedings of the 16th IFAC World Congress*, pp.1961-1966.

Nawrat, A. and Kuś, Z. (2013). Vision Based Systems for UAV Applications, *Vol. 481, Springer*, Switzerland.

Peng, C., Bai, Y., Gong, X., Gao, Q., Zhao, Ch. and Tian, Y. (2015), Modeling and Robust Backstepping Sliding Mode Control with Adaptive RBFNN for a Novel Coaxial Eight-rotor UAV. *IEEE/CAA Journal of Automatica*, 2(1), pp. 56-64.

Raptis, I.A. and Valavanis, K.P. (2011). Linear and nonlinear control of small-scale unmanned helicopters. Intelligent systems, control, and automation, *Science and engineering*, Vol.33., Springer, Dordrecht.

Sadalla T., Horla D. (2015a). Analysis of simple anti-windup compensation in approximate pole-placement control of a second order oscillatory system with time-delay, In *20th International Conference on Methods and Models in Automation and Robotics* (MMAR), pp. 1062-1066.

Sadalla T., Horla D. (2015b). Analysis of simple anti-windup compensation in pole-placement control of a second order oscillatory system, *Measurement Automation Monitoring,* 61(2), pp. 54-57.

Szafrański, G., Czyba, R. and Błachutra, M. (2015). Modeling and identification of electric propulsion system for multirotor unmanned aerial vehicle design, In *Proceedings of the 2014 International Conference on Unmanned Aircraft Systems (ICUAS 2014)*, Orlando FL, USA, pp. 470-476.

Valavanis, K.P. et al. (2007), Advances in Unmanned Aerial Vehicles. State of the art and the road to autonomy. *Intelligent systems, control, and automation, Science and engineering,* Vol.33., Springer, Dordrecht.